

Abstract S85 Table 1 30 and 90 day readmissions and A&E attendances by group

| | Declined to attend PEPR n = 34 | Completed PEPR n = 2 | p value (Chi ²) |
|----------------------------|-----------------------------------|-------------------------|-----------------------------|
| 30 day readmission%(n=) | 18% (n = 6) | 0% (n = 0) | p = 0.046 |
| 90 day readmission%(n=) | 29% (n = 10) | 5% (n = 1) | p = 0.031 |
| 30 day A&E attendance%(n=) | 15% (n = 5) | 0% (n = 0) | p = 0.072 |
| 90 day A&E attendance%(n=) | 38% (n = 13) | 5% (n = 1) | p = 0.007 |

2013, Thorax). We secured funding to pilot PEPR in our local DGH population. Here, we present the initial five months data. **Aims and objectives** This study aimed to investigate the impact of PEPR on exercise tolerance, QoL and health care utilisation in a local DGH population.

Methods Data were collected prospectively from successive patients referred for PEPR between December 2012 and May 2014. Outcome measures consisted of ISWT and QoL (CAT). Healthcare utilisation was measured through 30 and 90 day readmission and A&E attendance rates. Descriptive statistics and significance values were calculated in SPSS (version 22) using paired t-test and Chi².

Results 64 patients were referred to PEPR. 53% (n = 34) decline to attend, 15% (n = 10) failed to complete the programme. Subsequently 31% (n = 20) patients completed PEPR which is comparable to standard PR. Exercise tolerance was significantly improved (difference between the means 46 m 95% CI +/-33 m p = 0.009). QoL was significantly improved (difference between the means 5.4 95% CI +/-3.1 p = 0.002). Table 1 demonstrates the impact of PEPR on healthcare utilisation. Both 30 and 90 day readmissions were significantly reduced. 90 day A&E attendances were significantly reduced. Average LoS following readmission in the group who declined PEPR was 11 days compared to an average LoS following readmission in PEPR group of 1 day. Considering the savings associated with bed days alone and staffing expenses the cost benefit of PEPR was £21309 pa.

Conclusions Results suggest PEPR in a DGH population has a significant impact on QoL and exercise tolerance with reductions in healthcare utilisation and associated cost benefits.

Pulmonary infection: discovery science

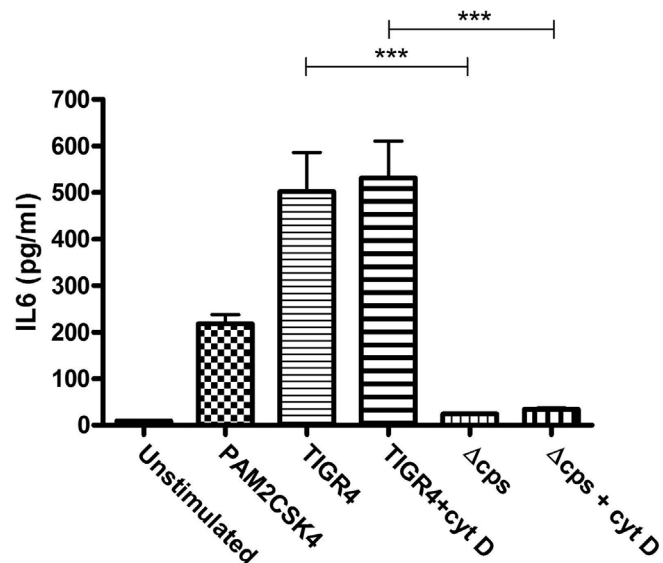
S86 THE INFLAMMATORY RESPONSE TO STREPTOCOCCUS PNEUMONIAE IS EXAGGERATED BY THE POLYSACCHARIDE CAPSULE

JN Periselneris, S Chimalapati, G Tomlinson, A Dyson, C Hyams, H Rukke, F Peterson, M Singer, M Noursadeghi, JS Brown. *University College London, London, UK*

10.1136/thoraxjnl-2014-206260.92

Streptococcus pneumoniae infections characteristically cause a high degree of inflammation. The *S. pneumoniae* polysaccharide capsule prevents opsonophagocytosis and is essential for virulence. The capsule might also be expected to reduce the host's inflammatory response by inhibiting bacterial interactions with pro-inflammatory signalling proteins eg toll-like receptors (TLR), but this has not previously been investigated. Using isogenic unencapsulated strains and *in vitro* and *in vivo* models of infection we have characterised capsule effects on the inflammatory response to *S. pneumoniae*.

Surprisingly, although the unencapsulated (Δcps) *S. pneumoniae* strain was much more sensitive to phagocytosis by



Abstract S86 Figure 1 Monocyte derived macrophages incubated with media or 10 μ M cytochalasin D for 30 min. Cells washed in PBS, then incubated with bacteria or controls for 6 h. Supernatants assayed for IL6 by ELISA

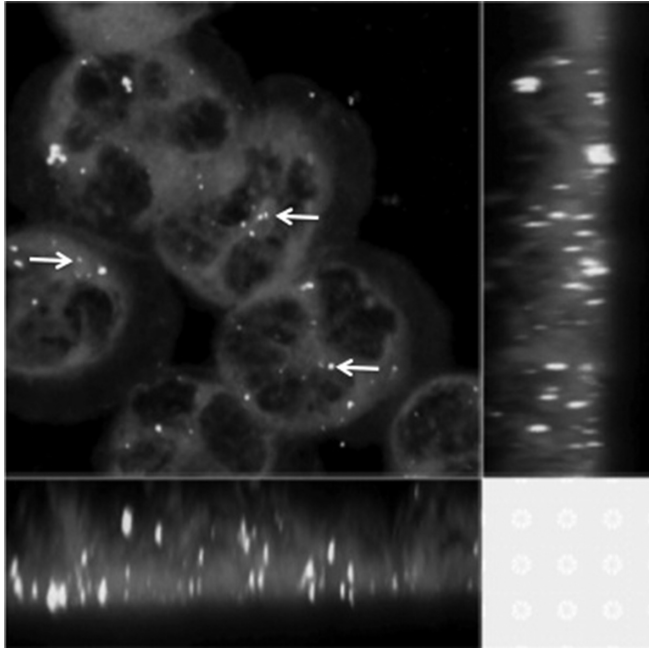
macrophages and induced a stronger NF κ B response by human monocyte derived macrophages (MDMs) it caused similar levels of stimulation of a TLR2 reporter cell line as the encapsulated strain TIGR4. In addition, microarrays demonstrated increased transcription of pro-inflammatory cytokines by MDMs in response to TIGR4 compared to the Δcps strain, and quantitative PCR and ELISAs confirmed stronger TNF, IL1 β , and IL6 responses by MDMs to TIGR4. Furthermore, compared to the Δcps strain the TIGR4 strain caused greater neutrophil recruitment and higher cytokine levels in the lungs in a mouse model of pneumonia, as well as higher serum cytokine levels with worse hypotension in a rat model of sepsis. Additional *in vitro* experiments excluded antibody, complement, pneumolysin, the inflammasome, and lectin-mediated signalling as mechanisms driving differences in inflammatory responses between TIGR4 and Δcps . Expression of the TIGR4 capsule in *Streptococcus mitis* did not increase MDM or murine inflammatory responses. Notably, preventing phagocytosis with cytochalasin D did not alter differences in the inflammatory response between TIGR4 and the Δcps strains, and *in silico* analysis suggested the Δcps strain activated a wider range of transcription factors.

Overall, the data indicate that unencapsulated *S. pneumoniae* stimulate a wider range of host cell signalling pathways than encapsulated bacteria, some of which are likely to be anti-inflammatory. Hence the capsule, rather than reducing inflammation, causes increased pro-inflammatory responses and subsequent disturbances to host physiology during *S. pneumoniae* infection. Targeting the mechanisms responsible for capsule-dependent inflammation could offer novel treatment options for reducing the morbidity and mortality associated with *S. pneumoniae* infections.

S87 A FUNCTIONAL COMPARISON OF NEONATAL AND ADULT NEUTROPHIL RESPONSES TO RESPIRATORY SYNCYTIAL VIRUS

¹GL Saint, ¹BF Flanagan, ¹R Corkhill, ²RL Smyth, ¹PS McNamara. ¹Institute of Women's and Children's Health, Liverpool, UK; ²Institute of Child Health, London, UK

10.1136/thoraxjnl-2014-206260.93



Abstract S87 Figure 1 Indirect fluorescent confocal microscopy was carried out on cytopins of neutrophils purified from adult blood and incubated with RSV for a 2 h in the presence of GM-CSF. Z stacks were taken using a Leica confocal and Z-projection images produced using Imaris software. RSV (white arrow) is identified in all depths of the cytoplasm in this orthogonal view throughout the cell in discrete packets suggestive of endosomes

Introduction and objectives Respiratory Syncytial Virus (RSV) is a major cause of lower respiratory tract infection during infancy. Neutrophils are the predominant cell type within the RSV-infected airway, 80% of inflammatory cells from BAL of intubated infants being neutrophils. Despite extensive research unpicking innate viral responses to RSV little is known about the specific role the neutrophil plays. The aim of this work was to investigate the response of neutrophils to RSV using an *in vitro* model utilising neutrophils from adult volunteers. To investigate whether relative immaturity of infant neutrophils leads to impaired responses we are now comparing adult neutrophils with neonatal neutrophils, isolated from cord blood.

Methods Highly purified neutrophils from whole blood of healthy adult donors were incubated with RSV. Samples were taken at 2, 4, and 20 h for QT-PCR of RSV N gene, western blot analysis and cytospin slides for confocal imaging of RSV F protein. Experiments were then replicated using neutrophils purified from cord blood, collected from the placenta following elective caesarean section, of healthy term neonates. Supernatants were stored for measurement of the cytokine response of the neutrophil to RSV.

Results Uptake of RSV by adult neutrophils was shown by both western blot and quantitative RT-PCR. Maximal uptake was at 4 h with a reduction by 20 h. Confocal microscopy was undertaken, using a primary monoclonal antibody to RSV fusion protein. This showed that RSV was internalised inside the cytoplasm in a distribution suggestive of endosomal uptake (*see figure*). Preliminary data suggests that neonatal neutrophils are also capable of this viral uptake but work is ongoing to determine differences between the two models.

Conclusions We have shown that neutrophils may be involved in viral clearance as part of the immune response to viral invasion. They appear to take up virus with kinetics suggestive of

endocytosis. Work is ongoing to establish the mechanism of entry using a panel of inhibitors. Initial results would suggest that neonatal neutrophils may respond similarly but work continues to establish whether this is the case and if there is any functional impairment that may explain infants' propensity to severe disease.

S88 ELECTRON TOMOGRAPHY DETECTS ULTRASTRUCTURAL ABNORMALITIES IN PATIENTS WITH PCD DUE TO A DNAH11 DEFECT

¹R Kwan, ²T Burgoyne, ³M Dixon, ²M Patel, ²J Scully, ²A Onoufriadis, ³C Hogg, ²HM Mitchison, ³A Shoemark. ¹Imperial College, London, UK; ²University College London, London, UK; ³Royal Brompton Hospital, London, UK

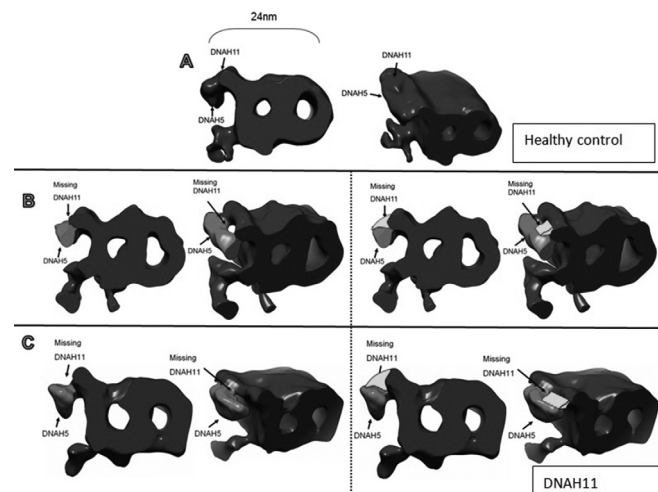
10.1136/thoraxjnl-2014-206260.94

Primary Ciliary Dyskinesia (PCD) is a genetically heterogeneous condition, characterised by impaired mucociliary clearance and chronic sino-pulmonary disease. Over 30 causative gene mutations resulting in dysfunctional ciliary motility and structure have been identified. Ciliary ultrastructure examined by Transmission Electron Microscopy (TEM) is currently the diagnostic gold standard. Patients with mutations in the gene *DNAH11* have a hyperfrequent ciliary beat and clinical symptoms of PCD. Diagnosis of a *DNAH11* defect by TEM is difficult due to apparently normal ciliary ultrastructure. The electron tomography technique, an extension of TEM, produces 3D models of cilia with superior resolution.

The aim of this study was to determine if electron tomography can detect ultrastructural abnormalities in patients with *DNAH11* defects.

Immunofluorescence by specific antibodies for *DNAH11* showed localisation to the proximal portion of cilia. Proximal cilia cross sections from araldite embedded nasal brush biopsies were examined. Dual axis tomograms were collected on a Philips CM200 electron microscope. The data were analysed using IMOD software and averaged using PEET.

Electron tomography and averaging of cilia cross sections indicated a deficiency in the outer dynein arm, consistent across



Abstract S88 Figure 1 Averaged microtubule doublets imaged using Chimaera. (A) normal control (B) and (C) *DNAH11* mutations with DNAH5 highlighted in red, showing the missing DNAH11 (left two images) and the proposed DNAH11 shapes inserted, coloured green (right two images)